An Optimized Control Scheme for Solar Energy Tracking Systems

Alaa M. Abdel-hamed[*], Almoataz Y. Abdelaziz[**], Yazan M Alsmadi[***‡]

[*] Electrical Power and Machines Engineering Department, High Institute of Engineering, El Shorouk Academy, Cairo, Egypt;
[**] Faculty of Engineering and Technology, Future University in Egypt, Cairo, Egypt;
[***] Department of Electrical Engineering, Jordan University of Science and Technology, Irbid, Jordan
(a.mohammed@sha.edu.eg, almoataz.abdelaziz@fue.edu.eg, ymalsmadi@just.edu.jo)
[‡] Corresponding Author: Yazan M Alsmadi, P.O.Box 3030, Irbid 22110, Jordan

ymalsmadi@just.edu.jo

Received: 10.05.2022 Accepted: 16.07.2022

Abstract- This paper proposes a Harris Hawks Optimization (HHO) algorithm for an efficient single-axis solar tracking system. The primary goal of the tracking system is to improve the performance of solar energy conversion systems. To achieve this target, the proportional-integral-derivative (PID) controller, optimized by the HHO, is employed for controlling single-axis sun-tracking control systems. The Weighted Goal Attainment Function (WGAF) combines various individual performance indices, namely Integrated-Squared Error (ISE), Integrated-Time-Weighted Absolute Error (ITAE), and Integrated-Absolute Error (IAE). Its impact on the system performance is employed using different weighting factors representing other system priorities. The performance of the proposed control scheme is verified for variable sun positions and load torque. The HHO-PID controller, optimized using the WGAF, is compared with the conventional PID-controller's overall system performance. The results obtained from HHO-PID, using the WGAF, are compared to those obtained using ISE, IAE, and ITAE. Analysis results have shown that the lowest fitness function level is obtained (0.14076) using the proposed improved fitness function, compared with other individual fitness functions, which are 1.4386, 5.44438, and 0.4214 for ISE, IAE, and ITAE, respectively. Also, results have shown that the proposed improved fitness function has the best rising time (0.085 sec), settling time (0.16 sec), percent steady-state error (0.00061), and percent overshot (0.00227). The simulation findings also validate the proposed scheme and the effectiveness of the HHO-PID controller, tuned by the WGAF. The results show that the proposed tuned controller has a superior performance in terms of robustness and control effects on the setting time, maximum overshoot, and steady-state error.

Keywords Solar Tracking, Optimal Control, Harris Hawks Optimization (HHO) Algorithm, Weighted Goal Attainment Function

1. Introduction

Among the various types of natural energy resources, renewable energy (RE) is a type that can easily be transformed into available energy forms. This type of energy includes solar, wind, biological processes, flowing water, and geothermal activity. The fact that fossil fuel resources are being rapidly depleted, causing climate change, and polluting the environment has made the use of renewable energy sources grow quickly. Another important factor increasing the implementation of RE sources is that they can be installed extensively and expanded using diverse technologies [1], [2], [3]

Solar energy is a more accessible form of energy for obtaining clean electrical power. It is less harmful and has lower economic costs than other sources of RE. However, the efficiency of solar cells is only about 20%. This efficiency has a limited capacity to generate efficient electrical energy from the sun's energy at full solar efficiency [3]. Therefore, the control of sun-tracking has emerged as a way of maximizing the efficiency of electrical energy derived from sunlight [4].

The sun-tracking control system is one of the efforts that have been developed to improve the efficiency of solar panels. This control system aims to track sun panels at complete efficiency throughout the day. This takes place by allowing rays from the sun to arrive perpendicular to the solar panels. Two tracking control systems are available in the literature: one-axis and two-axis systems [5].

Several studies have been conducted to develop solar-tracking Photovoltaic (PV) systems. Recently, several studies have aimed at the development of sun-tracking control systems. New research is being developed to make sun rays perpendicular to the solar panels using several control

techniques. According to these studies, the implementation and applications of solar/sun energy have increased rapidly in the last few years, and new methods and materials are being developed and investigated for this source of energy [2], [5]–[9]

According to one estimate, up to 95% of the control loops in the process industry are proportional integral derivative (PID) control loops. Their wide application in the process control industry is since their model is considered to be simple and can be easily grasped by process operators [7], [10]-[14]. Three elements—the proportional gain (K_P), derivative gain (K_D), and integral gain (K_I)—represent a typical structure for the general PID controller. Usually, tuning a PID controller is considered a trial-and-error method. It depends on the user's expertise, and due to changing system dynamics, they are tuned poorly. The tuning methods of conventional PIDs, such as Cohen–Coon and Ziegler–Nichols, are widely used. However, these approaches do not offer the most efficient or optimum tuning parameters [15]-[16].

Recently, several research breakthroughs have been accomplished in artificial intelligence-based optimization methods for solving various types of problems: Particle Swarm Optimization (PSO), the Bacterial Foraging Algorithm (BFA), the Firefly Algorithm (FFA), the Cuckoo Search Algorithm (CSA), and Ant Colony Optimization (ACO), which are reported in [11], [17]-[20], respectively.

In [21], a two-axis solar tracker's performance is modeled and controlled using AI via MATLAB software and Real-Time Workshop tools. To build a solar tracker, a neural network-based identifier is proposed, trained, and validated. With and without a self-tuning FL controller, PIDs are used to control the tracker system. This study concluded that the choice of a neural network via the training and validation process depends on several factors, such as the amount of representative training data and the selection of these data. Moreover, choosing the activation functions and the size of nodes per hidden layer of initial weights should be considered. Training stopping methods and error evaluation are essential factors in improving the network estimation and generalization. This work proved that PID controllers with and without self-tuning FLCs provide commendable performance in acting as a controller of the solar-tracker system. In addition, the FLC's self-tuning controllers always generate better performance than the normal FL-PID. Both fuzzy controllers allow better performance than the conventional PID controller. When the control process is under stable conditions, the PID controller works well, but its performance decreases in the presence of disturbances.

In [22], a PSO-PID control system controls a solar tracking system. It is built to optimize the existing PID control. The system is designed to be able to track the sun's position. In [23], a design for a single-axis sun-tracking system is carried out based on a PID controller and a fuzzy logic-controlled system. The control system is built on an Atmel micro-controller. MATLAB simulation is used as the software installed into the control units. This paper proves that fuzzy controllers are more efficient than PID controllers in single-axis sun-tracking control systems. At the same time, a processing system of maximum efficiency is determined by considering the two controllers of the implemented system.

In [24], a fuzzy logic (FL)-based sun-tracking system is proposed for optimizing the operation of solar energy receivers. The results obtained showed good performance for the FL control systems. It was found that the setting time for FL controllers and PI controllers is approximately the same, but the FLC controller shows less maximum overshoot. The main benefit of this designed control is that it has fewer ripple values in the transient period.

Several efforts are being carried out in the literature to improve and enhance the optimization methods developed for solving various problems in engineering and science [25]-[27].

In [28], a machine vision control technique for a sun-tracking system is proposed. The goal is to track the sun's centroid dynamically under low irradiation and with high flexibility. The sun-tracking system is designed to work independently without the manual setup for the location's spatiotemporal data. The measurement indicated that the sun's centroid tracking precision of the suggested tracker with Al (α) and Az (γ) is 0.66º and 0.23º, respectively, with the solar position algorithm while 0.65º and 0.59º, respectively. The results show that the implemented system can measure accurately with the same tracking performance compared with the two-established measurements. The suggested control system can meet the requirements for a flexible control system for proposed parabolic dish solar concentrators.

In [29], a new application of an efficient Adaptive Sine Cosine Algorithm (ASCA) is proposed for determining the optimal settings for the PID controllers in a hybrid renewable energy system. The ASCA is suggested for enhancing the searching capabilities of the traditional SCA and its stagnation to local optima. The proposed system consists of three sources PV, wind turbine, and battery storage. A DC/DC boost converter is used to convert the DC voltage to an AC voltage through an inverter of a 3-phase type. The considered fitness function is expressed in terms of the voltage and current errors for enabling the HRES to participate well within the connected micro-grid through optimal parameters of the PID controllers. Obtained results verify that the HRES's performance is enhanced by optimizing the gains of the HRES controllers by using the ASCA under various operating conditions of sun temperature, irradiation, and wind speed. The proposed PID controllers enhance the system performance where the output current, voltage, and power fluctuations have been alleviated. ASCA is superior for assigning the gains of the PID controller in terms of the fitness function and the convergence characteristics.

Several efforts are carried out in the literature to improve and enhance the optimization methods that were developed for solving various problems in engineering and science. One of these methods is the Harris's Hawks Optimization (HHO) method described in [30]. As HHO is characterized by its competitive performance compared with other optimization algorithms, several applications of HHO are now seen in power systems. In [31], a modified HHO was developed to find optimal settings for damping a power system's oscillation

and provide an optimal controller design. In [32], an assessment study comparing two optimization algorithms, JAYA and HHO, is carried out to solve the coordination problems of directional overcurrent relays. In [33], the HHO algorithm was developed to control the DC motor speed by finding the optimal parameters of a PID controller. In [34], a multi-objective HHO algorithm was developed to optimize the Fractional Order PID (FOPID) controller parameters applied to the governing system of a hydraulic turbine. In [35], HHO was used to enhance the performance of a DVR controller. An AVR system was optimized and operated with the optimal PID design employed by the HHO algorithm in [36]. The HHO algorithm was applied in [37] to find the optimal tuning of a FOPID controller in a DC-DC buck converter. The HHO algorithm was developed for the parameter estimation of solar cells and Proton-exchange Membrane Fuel Cells (PEMFC) in [38] and [39], respectively.

The current paper proposes an optimization scheme that uses the HHO algorithm to improve the performance of single-axis sun-tracking systems. The fitness function is mathematically modeled and designed using a proposed WGAF. The performance of the proposed control scheme is verified in the case of variable sun position and variable load torque using the same controller. The HHO-PID controller optimized using the WGAF is compared with conventional PID controllers. It is also compared with an HHO-PID controller optimized using the Integral Square Error (ISE), Integral Absolute Error (IAE), and Integral time square error (ITAE) performance indices used in the literature.

The salient features of this paper can be ordered as follows:

1. It proposes an HHO algorithm-based single-axis sun-tracking control system.
2. It develops a new fitness function for tuning PID controllers. This fitness function combines the system performance indices.
3. It assesses the system performance of combined and individual system performance indices.
4. Applications to two studied cases are employed to verify the proposed controller.

2. Complete System Modeling

2.1. Sun Tracker Modeling

Solar energy conversion is a way of transforming the sun's rays into utilized electrical or heat energy. PV cells are used to obtain electrical power. The technology used for manufacturing PV cells determines their efficiency. The cells' output efficiency is not initially very high, but it can be increased by using sun-tracking systems, which are electro-mechanical systems. These systems assure that the sun's radiation remains perpendicular to the cells during the day. In general, the efficiency of PV cells can be maximized by increasing the output efficiency of the PV cell itself using effective control algorithms, such as MPP tracking, to increase the output power [25].

There are three categories of sun trackers: passive, time-based, and active. The operating principle of passive trackers depends on an imbalance that results in pressure differences created at each end of the tracker [26]. In time-based trackers, daily and yearly solar positions are programmed into an algorithm. In active trackers, the sun's position is measured by sensors, and a specific signal is generated.

A schematic diagram of a single-axis sun-tracking control system is presented in Fig. 1. This tracking system consists of two permanent magnet motors, two-directional light-detecting circuits, and two amplifiers for driving the motor system. The two-drive Permanent Magnet DC (PMDC) motors are decoupled so that the angle of rotation of one motor does not affect that of the other PMDC motor, minimizing control problems. This implementation will reduce the system's power consumption, increase efficiency, and increase the total amount of generated electricity [26].

The azimuth angle is controlled by PMDC motors, while the tilt angle is assumed to be constant. PID controllers achieve the control of PMDC motors. These controllers are optimized using conventional techniques and one of the swarm intelligence-based algorithms, i.e., the HHO algorithm. The proposed tracking system uses sun-tracking dynamics sensors to determine the sun's position, then generates a reference command signal for the PID control. This reference error is processed using the PID controller. The PID controller produces a command for the rotation of the PMDC motors. This paper emphasizes the optimum tuning for a PID controller for a single-axis PMDC motor, considering it an optimization problem.

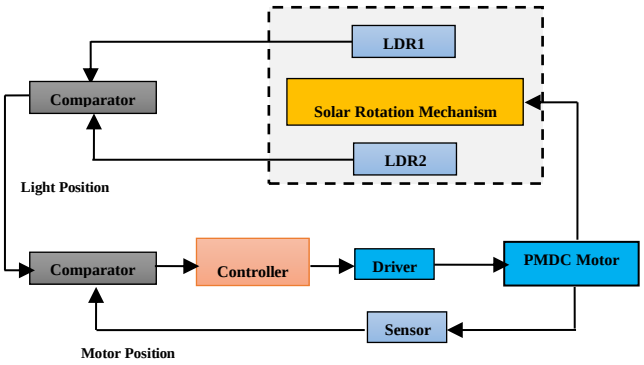

Fig. 1. Sun tracking control architecture

2.2. Amplifier and Photo Detecting Modeling

The amplifier and photo-detecting circuit create an electrical driving force for the PMDC motor. The developed driving force is proportional to the panel's rotating misalignment of the light source. These circuits are considered a single variable, P, where P is the proportionality constant measured in (volts/radian). The value of P represents the photodetector circuit's gain, which adjusts the circuit [24].

2.3. Permanent Magnet DC Motor

The solar panel is actuated using a PMDC motor. In this section, a PMDC motor is modeled using MATLAB/Simulink GUI Environment. Differential equations for the armature current and the angular speed are arranged as a state-space representation, as Equation (1) indicates [24].

$$\begin{bmatrix} i^{\cdot}(t) \\ \omega^{\cdot}(t) \end{bmatrix} = \begin{bmatrix} -\frac{R}{L} & -\frac{K}{L} \\ \frac{K}{J} & -\frac{B}{J} \end{bmatrix} \cdot \begin{bmatrix} i(t) \\ \omega(t) \end{bmatrix} + \begin{bmatrix} \frac{1}{L} & 0 \\ 0 & -\frac{1}{J} \end{bmatrix} \cdot \begin{bmatrix} V(t) \\ T_L(t) \end{bmatrix} \quad (1)$$

where V is the applied voltage, K is the motor constant, J represents the rotor inertia, B represents the viscous damping, T_L is the torque delivered to the load, L represents the inductance of the armature, R is the armature resistance, and I is the armature current.

The parameters of the various terms in Eq. (1) are defined with the values identified in Table 1. A schematic block diagram of the PMDC motor is shown in Fig. 2.

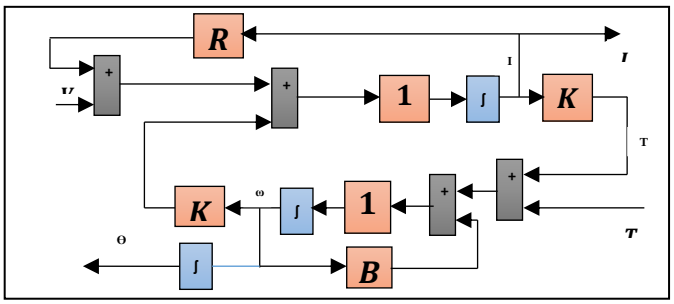

Fig. 2. Simulink Model for PMDC motor

Table 1. PMDC motor parameters

Motor Parameters	Values
Resistance R	0.5Ω
Inductance L	0.13H
Inertia J	3.7e-5 Kg.m^2
Torque constant K_t	0.1098 Nm. /A
Back emf constant B	0.01 Nm.

3. Harris Hawks Optimization Algorithm (HHO)

Haidari et al. [40] developed the HHO algorithm, which was inspired by the cooperative action of Harris's Hawks' chasing style. Some hawks try to surprise their prey, swooping cooperatively on it from different directions. Moreover, Harris's Hawks can choose between different chase patterns depending on various patterns and scenes of prey flight. HHO has three main phases. These phases are studying prey, surprising it with a pounce, and the many types of Harris's Hawks' attacking strategies. Each phase of the three patterns is described in the following subsections [40], [41].

3.1. Exploration Phase

In HHO, the Harris's Hawks perch on random locations and wait to detect prey by depending on two strategies:

$$X(it+1) = \begin{cases} X_{rand}(it) - r_1|X_{rand}(it) - 2r_2X(it)| & q \geq 0.5 \\ X_{rabbit}(it) - X_m(it) - r_3\big(LB + r_4(UB - LB)\big) & q \geq 0.5 \end{cases} \quad (2)$$

where $X(it)$ is the current-position vector of the hawks; $X(it+1)$ is the position vector used in the next iteration it; $X_{rabbit}(it)$ is the rabbit's position; q, r_1, r_2, r_3, and r_4, are random numbers between [0,1], which are all updated in every iteration; LB and UB show the variables' upper and lower bounds; $X_{rand}(t)$ is a hawk that is randomly selected from the population; X_m is the average hawk's position in the current population. The average position of the hawks is attained using Eq. (3):

$$X_m(it) = \frac{1}{N}\sum_{i=1}^{N} X_i(it) \quad (3)$$

where $X_i(it)$ denotes the location of every hawk in the iteration it, and N gives the total number of hawks.

3.2. Conversion from exploration to exploitation

To model this phase, the rabbit energy is modeled as:

$$E = 2E_o\left(t - \frac{it}{T}\right) \quad (4)$$

where E represents the prey-escaping energy, T represents the maximum iteration number, and E_0 is the initial state of its energy.

3.3. Exploitation phase

i. Soft Besiege ($r \geq 0.5\ and |E| \geq 0.5$)

This method is modeled by using the following principles:

$$X(it+1) = \Delta x(it) - E|JX_{rabbit}(it) - X(it)| \quad (5)$$

$$\Delta x(it) = X_{rabbit}(it) - X(it) \quad (6)$$

where $X(it)$ is the difference between the current position and the position vector of the rabbit in the iteration it, r_5 is a random number between [0,1], and $J = 2(1\text{-}r_5)$ represents the rabbit's random jump strength throughout the escaping process. The J value varies randomly in every iteration to simulate the nature of rabbit motions.

ii. Hard besiege ($r \geq 0.5\ and |E| < 0.5$)

In this method, current positions are updated by using Equation (7):

$$X(it+1) = X_{rabbit}(it) - E|\Delta X(it)| \quad (7)$$

iii. Soft besiege with progressive-rapid dives ($|E| \geq 0.5\ and\ r < 0.5$)

The following equation demonstrates how the hawks can decide next:

$$Y = X_{rabbit}(it) - E|JX_{rabbit}(it) - X(it)| \quad (8)$$

According to LF-based patterns, they will dive using the following rule:

$$Z = Y + S \times LF(D) \quad (9)$$

Where D indicates the problem dimension, S indicates a random vector of dimension $1 \times D$, and LF represents the levy flight function. This function can be calculated as follows:

$$LF(x) = 0.01 \times \frac{u \times \sigma}{v^{\frac{1}{\beta}}},\ \sigma = \left(\frac{\Gamma(1+\beta) \times \sin\left(\frac{\pi\beta}{2}\right)}{\Gamma\left(\frac{1+\beta}{2} \times \beta \times 2^{\left(\frac{\beta-1}{2}\right)}\right)}\right)^{\frac{1}{\beta}} \quad (10)$$

where u, v represent random values between [0,1] and β represents a default constant, which is usually 1.5.

Therefore, the last strategy to update the hawks' positions in the soft besiege is expressed as follows:

$$X(it+1) = \begin{cases} Y\ if\ F(y) < F(X(it)) \\ Z\ if\ F(Z) < F(X(it)) \end{cases} \quad (11)$$

where Y and Z are determined using Eqs. (8) and (9)

iv. Hard besiege with progressive rapid dives ($|E| < 0.5 \; and \; r < 0.5$)

If |E| <0.5 and r <0.5, the rabbit has not have sufficient energy to escape, and a hard besiege stage is constructed before catching and killing the prey by the surprise pounce. This step on the prey side is the same as in the soft besiege, but the hawks try decreasing the distance of their average location with escaping prey. The following rule is performed in this case:

$$X(it+1) = \begin{cases} Y \; if \; F(y) < F(X(it)) \\ Z \; if \; F(Z) < F(X(it)) \end{cases} \quad (12)$$

where Y and Z are obtained using new rules in Eqs.(13) and (14).

$$Y = X_{rabbit}(it) - E|JX_{rabbit}(it) - X_m(it)| \quad (13)$$

$$Z = Y + S \times LF(D) \quad (14)$$

where $X_m(it)$ is obtained by Eq. (3). Z or Y will be the next location in the new iteration.

4. Design Of Controller Procedure

The proposed design procedure of the PID controller is dependent on developing the HHO that finds the best PID parameters. At the same time, the objective function varies from individual to combined performance indices. The following subsections describe the proposed integrated fitness function and solution methodology.

4.1. Objective Function

This paper adopts the proposed Weighted Goal Attainment Method (WGAF), as given in [42]. Eqs. (15)–(17) show the ISE, IAE, and ITAE fitness functions used for controlling the solar tracking system [43], [44].

$$F_1 = ISE = \int_o^{T\max} [\Delta\theta]^2 \, dt \quad (15)$$

$$F_2 = IAE = \int_o^{T_{\max}} |\Delta\theta| dt \quad (16)$$

$$F_3 = ITAE = \int_o^{T_{\max}} t \, |\Delta\theta| dt \quad (17)$$

Equation 18 demonstrates the proposed WGAF performance index, which will be minimized with HHO optimization techniques. This objective function shows an enhanced optimization problem domain compared with other stated fitness functions. The WGAF can satisfy the requirements of the designer by choosing a suitable α value. The value of α is greater than 0.7 for reducing the steady-state error and overshooting d. In contrast, α is set lower than 0.7 for reducing the rising and setting time [43].

$$F_4 = WGAF = e^{-\alpha}(t_s - t_r) + (1 - e^{-\alpha})(M_P + \Delta\theta) \quad (18)$$

where $\Delta\theta$ is the position deviation between the sun and the solar cell. α is a positive constant. The value of α is chosen such that ($\alpha \geq 0$) according to prioritizing the importance of the maximum overshot, the steady-state error, or the setting time and rising time. In this study, α-values from 0 to 1.5 are attempted, as indicated in the results section of this paper.

4.2. Implementation of HHO-PID Controllers

Equations (15)–(18) present various fitness functions of the designed PID controllers. They are solved by the proposed HHO to improve the dynamics of solar tracking control systems. The proposed solar tracking controller block diagram using the HHO-PID is shown in Fig. 3. According to the trials, the parameters of the HHO used in this optimization problem are indicated as 100, 20, and 1.5 for the number of search agents, the number of iterations, and default constant β, respectively.

5. Simulation Results

This model of a sun-tracking system is designed and simulated using MATLAB/SIMULINK models. The MATLAB/SIMULINK (The Math Works, Natick, Massachusetts, USA) schematic diagram of the solar tracking is shown in Fig. 4. Table 1 tabulates the complete data. The analysis was executed by running the system for 10 seconds. At this time, the sun-tracking control system was put under the reference position input of 100 rad/seconds at no load.

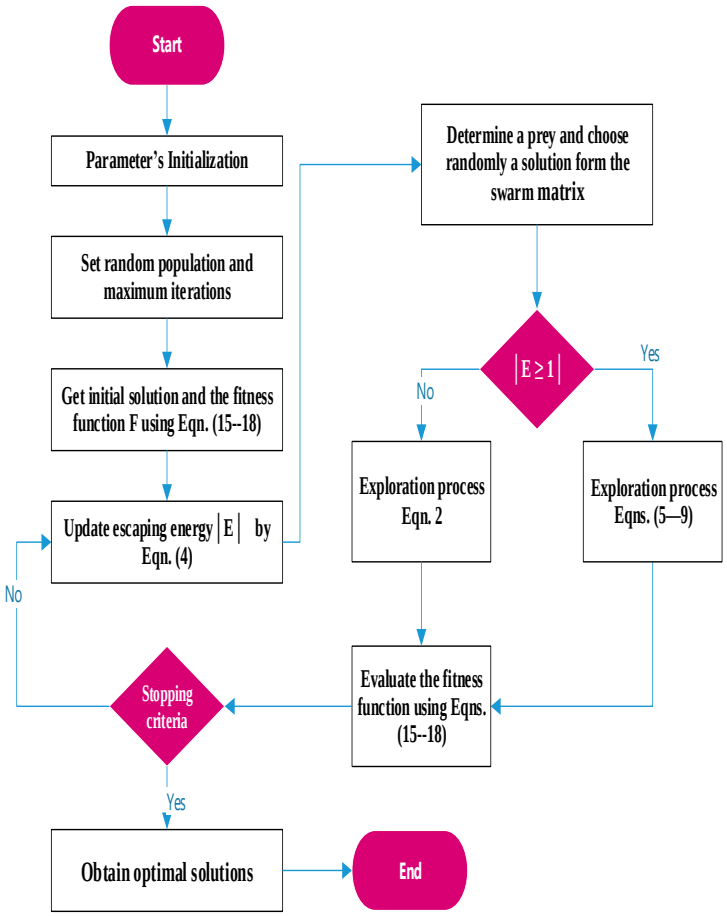

Fig. 3. HHO Algorithm Chart

5.1. System Response with PID Controllers Tuned Conventionally

Fig. 5 shows the dynamic system response for a classical PID controller. The settings of the conventional controller parameters are as follows: the proportional gain (K_P) is set to 3, the integral gain (K_I) is set to 1, and the derivative gain (K_d) is set to 0.02. As shown, the system presents oscillatory position behavior.

Table 2. Response parameters HHO-PID controller using WGAM

α	K_p	K_i	K_d	M_p%	t_r (s)	t_s (s)	e_{ss} %	Fitness value
0	1.88007	0.14940	0.09155	1.85070	0.1	0.14500	-0.1605	0.04500
0.2	1.96920	0.27691	0.10685	1.08198	0.090	0.145	0.00010	0.09575
0.4	1.98100	0.27900	0.12340	0.00227	0.0850	0.16	0.00061	0.14076
0.6	1.84496	0.25879	0.11177	0.05868	0.095	0.17	-0.00010	0.16202
0.8	1.75752	0.24643	0.10547	0.08363	0.105	0.18	-0.00012	0.19860
1	1.96468	0.27457	0.12230	0	0.09	0.16	-0.00085	0.21512
1.2	1.892444	0.26471	0.12035	0	0.09	0.175	-0.00062	0.24071
1.4	1.92001	0.26778	0.13981	0	0.09	0.220	-0.00095	0.32003
1.5	1.48164	0.20796	0.08792	0	0.13	0.22	0.00048	0.37686

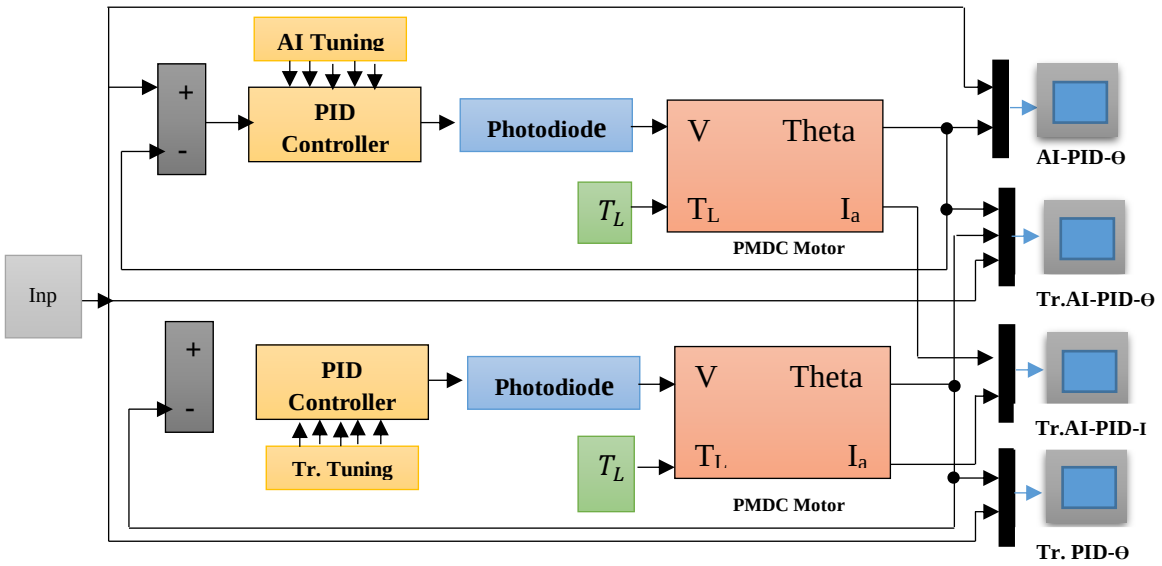

Fig. 4. SIMULINK model for the single axis *solar tracker*.

5.2. Position Response with PID Controller Tuned By HHO

The HHO-PID controller is implemented using the proposed WGAF, as indicated. The simulation results, which show the parameters of the optimum PID controller and the parameters of the related responses for different values of α (α = 0, 0, 2, … 1.5), are summarized in Table 1. The PID parameters, K_p, K_i, and K_d, are reported in Table 2 along with the system performance, measured by the overshot percentage, rise/setting times, and steady-state error. The controller parameters, K_p, K_i, and K_d, vary from 1.48164, 0.14940, and 0.09155 to 1.981, 0.279, and 0.13981, respectively. Figure 6 shows the system's responses for different levels of α: α = 0, α = 0.8, and 1.5. The lowest overshot percentage occurs at the highest level of α. It can be concluded that as the value of α increases, the value of the overshoot of the response decreases, but the rising and setting times increase, and vice versa.

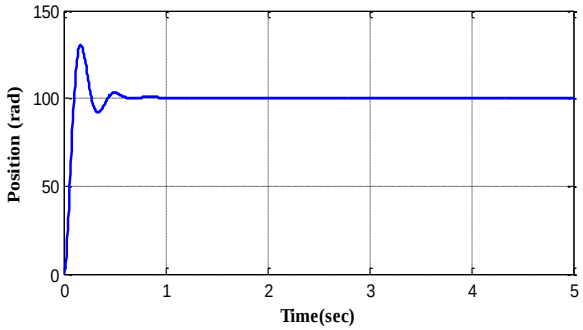

Fig. 5. System response using classical PID Controller

Table 3. Classical PID and HHO-PID controllers with different objectives

	Individual performance fitness functions				Proposed improved fitness function F_4		
Response & PID Parameters	Classical	ISE F_1	IAE F_2	ITAE F_3	WGAF (α =0.8)	WGAF (α =0.6)	WGAF (α =0.4)
K_P	3	1.99514	1.99753	1.71032	1.75752	1.84496	1.98100
K_I	1	0.95278	0.27891	0.23984	0.24643	0.25879	0.27900
K_D	0.02	0.99884	0.20349	0.08230	0.10547	0.11177	0.12340
Fitness function Val.	0.1912	1.43868	5.44438	0.42140	0.1986	0.16202	0.14076
Rising time(sec)	0.07	0.01500	0.07500	0.11000	0.105	0.095	0.0850
Overshot %	32.87347	27.65278	0.00016	1.94056	0.08363	0.05868	0.00227
Settling time (sec)	0.5850	0.67500	0.3200	0.16000	0.18	0.17	0.16
Percentage Steady state error%	-0.000002	-0.000037	-0.00005	-0.00043	-0.00012	-0.00010	0.00061

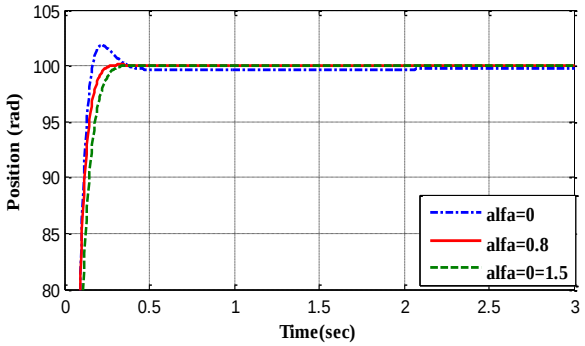

Fig. 6. System response using HHO-PID with WGAF

5.3. Controller performance with different objectives

To show the advantage of the proposed HHO-PID controller optimized using the WGAF, the results were compared to those obtained using the HHO-PID approach for the error criteria (IAE, ISE, and ITAE performance indices) indicated in Eqs. (15)–(17). The efforts of the solar tracking system using HHO-PID controllers optimized at α = 0.4 and the different fitnesses are shown in Table 3. By using the proposed improved fitness function, the lowest fitness function levels are obtained (0.14076) compared to other individual fitness functions, which are 1.4386, 5.44438, and 0.4214 for ISE, IAE, and ITAE, respectively. In addition, the time responses are indicated in Fig. 7. It is concluded that the HHO-PID controller with the WGAF proves to be more efficient than the classical controller and the HHO-PID controller using IAE, ISE, and ITAE with respect to the desired performance indices.

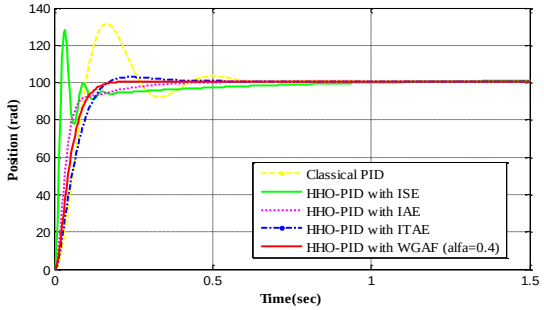

Fig.7. System response using HHO-PID with different fitness functions

5.4. Proposed Control Scheme Verification

Two verification cases were employed to prove the capability of the proposed HHO-PID controller. These two cases are applied for variable angular and load torque.

Case 1: Variable Angular Position

Case 2: Variable Load Torque

5.4.1 Verification results for Case 1

The system was subjected to a variable angular position to demonstrate the adaptive property of the HHO-PID controller with a WGAF fitness function. Figures 8 and 9 show the dynamic system responses for the error in the variable reference command considering the classical PID and HHO-PID controllers optimized using the WGAF.

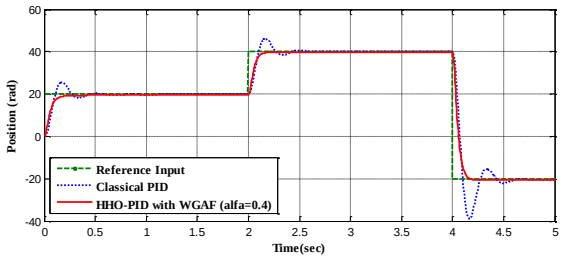

Fig. 8. The output of the system from classical and HHO-PID with WGAF

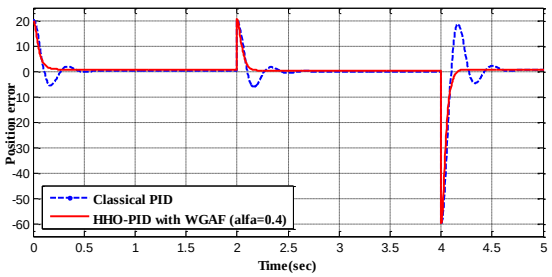

Fig. 9. The change of the error in variable reference input for classical and HHO-PID

Table 4. Verification of classical PID and HHO-PID controllers with different objectives

	Individual performance fitness functions				Proposed improved fitness function F_4
Response & PID Parameters	Classical	ISE F_1	IAE F_2	ITAE F_3	WGAF (α =0.4)
K_P	3	1.99514	1.99753	1.71032	1.84496
K_I	1	0.95278	0.27891	0.23984	0.25879
K_D	0.02	0.99884	0.20349	0.08230	0.11177
Fitness function Val.	-0.03868	10.62479	8.36927	10.13871	8.65150
Rising time(sec)	0.07	0.0150	0.06500	0.10500	0.0800
Overshot %	31.44133	28.14398	0.65051	2.99374	0.49930
Settling time (sec)	2.130	0.58000	2.0750	2.1850	1.140
Percentage steady state error %	-0.03868	0.018	-0.02009	-0.02261	-0.0200643

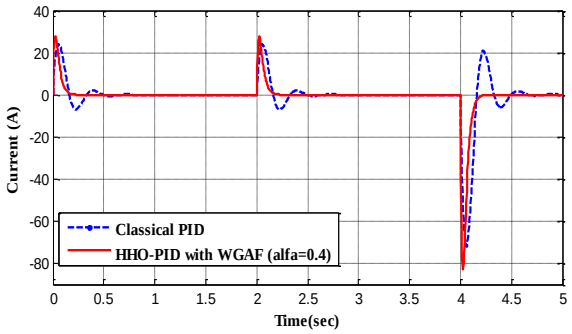

Fig.10: The motor current from classical and HHO-PID controllers for a load of 0 N

Although there are rough differences during the transient period of positions, both controllers follow the variable reference command. Figure 8 shows that the HHO-PID controller tuned with the WGAF gives better results with respect to overshoot, rise time, setting time, and other performance indices than all other controllers. Moreover, Fig. 9 shows that the error response in the case of the HHO-PID controller tuned with the WGAF is better. It can also be observed from Figure 9 that the error in the sun's angular position falls to zero very quickly in the case of the HHO-PID controller when compared with the reference command. However, each controller shows different transients in the current responses. As depicted in Fig. 10, the current has lower ripple magnitudes in the transients using the HHO-PID controller tuned with the WGAF than it does with the classical PID controller.

5.4.2 Verification results for Case 2

For the second case, Case 2, a variable load of changing values, shown in Fig. 11, is employed on the motor shaft. Fig. 12 shows the dynamic responses of the classical PID controller and HHO-PID controllers tuned by the proposed WGAF for variable reference commands. Table 4 shows the verification results of the proposed sun-tracking controller using the classical PID controller, the HHO-PID controller tuned by the proposed objective at α = 0.4, and the PID controllers tuned by different fitness values. Fig. 13 shows the change in the errors in the variable reference input for both a variable load is applied to the motor shaft, it is evident that the HHO-PID controller gives better results than the classical PID controller. Moreover, when the load implemented on the shaft of the motor increases, the system error also increases. Fig. 14 indicates the current response, which has a lower magnitude of transient ripples using the HHO-PID controller than the classical PID controller.

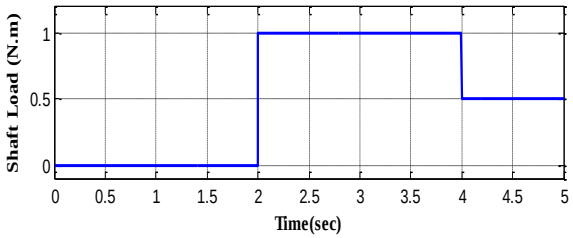

Fig. 11. Variable load applied to the motor shaft

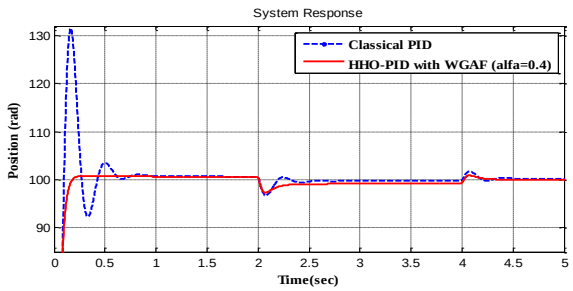

Fig. 12. The output of the system from classical and HHO-PID with WGAF at variable load

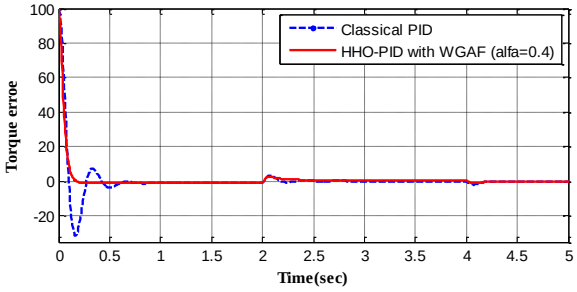

Fig. 13. The change of the error in variable load torque for both controllers

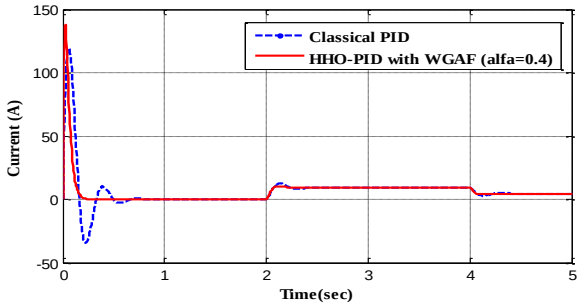

Fig. 14. The motor current from both controllers for variable load

6. Conclusion

This paper has developed an HHO-PID control scheme for designing solar tracking systems in the MATLAB/SIMULINK environment. the proposed HHO-PID controller is compared with the PID-tuned controller using different individual objectives with defined performance indices. The simulation results achieved better performance for the proposed HHO-PID controller integrating the WGAF. The verification cases show that the proposed scheme using the HHO-PID controller, under variable positions and shaft loads, has lower magnitudes of transient ripples. Practically, the obtained results prove that the proposed controller enhances the time-response speed. The framework presented for single sub-tracking control systems was executed in the hardware in this study. It is a very efficient and cost-effective solution for single-axis sun trackers. In the long run, it will be helpful to provide an efficient control system that will be able to minimize the energy crisis in many countries. In addition, the proposed design can utilize solar-powered autonomous sea vehicles, solar-powered space stations, and automatically aligned large telescopes. All of these practical systems need an accurate alignment with solar irradiation to optimize energy gain from the sun. In the future, the proposed control scheme can be modified and extended to be more intelligent to meet the challenge of the rapidly growing social demand for solar energy.

References

[1] A. Renuka Prasad and S. Singh, "Importance of Solar Energy Technologies for Development of Rural Area in India", International Journal of Scientific Research in Science and Technology, Vol. 3, Issue 6, pp. 585-599, 2017.

[2] S. Das, P. Sadhu, N. Pal, and A. Mukherjee, "Single Axis Automatic Solar Tracking System Using Microcontroller", Vol. 12, No. 12, pp. 8028 - 8032, 2014.

[3] A. BaAy and Bahadir, "Investigation of Energy Generation at Test System Designed by Use of Concentrated Photo-Voltaic Panel and Thermoelectric Modules", International Journal of Renewable Energy Research(IJRER), Vol.8, No.4, pp. 1859-1867, 2018.

[4] M. Green, K. Emery, D. King, and S. Igari, "Solar cell efficiency tables" Progress in Photovoltaics: Research and Applications, Vol.8, pp. 187–196, 2000.

[5] M. Ali and J. Suharsono, "Optimization on PID and ANFIS Controller on Dual Axis Tracking for Photovoltaic Based on Firefly Algorithm", International Conference on Electrical, Electronics and Information Engineer, Denpasar, Bali, Indonesia, 2019.

[6] D. Shugar, T. Hickman, and T. Lepley, "Commercialization of a value engineered photovoltaic tracking system", In 25th IEEE PVSC proceedings, pp. 1537–1540, May 1996.

[7] M. Chowdhury, A. Khandakar, B. Hossain, and R. Abouhasera, "A Low-Cost Closed-Loop Solar Tracking System Based on the Sun Position Algorithm", *Journal of Sensors*, vol. 2019, pp.1-11, 2019.

[8] A. Benhadouga, I. Colak, M. Meddad and A. Eddiai, "Experimental Validation of The Sliding Mode Controller to Improve the efficiency of the MPPT Solar System," 2021 10th International Conference on Renewable Energy, 2022.

[9] W. Al Abri, R. Al Abri, H. Yousef, and A. Al-Hinai "A Global MPPT Based on Bald Eagle Search Technique for PV System Operating under Partial Shading Conditions",10th International Conference On Smart Grid , 2022.

[10] F, Issi, and O. Kaplan, "Simulation of a Wireless Charging Multiple EScooters using PV Array with Class-E Inverter Fed by PI Controlled Boost Converter for Constant Output Voltage", 10th IEEE International Conference on Smart Grid,2022.

[11] M. Muhammad S. Ali, "Optimal PID controller design through swarm intelligence algorithms for sun tracking system", Applied Mathematics and Computation, Elsevier Vol. 274, pp. 690–699, 2016.

[12] M. Abdelwanis and R. El-Sehiemy, "Performance enhancement of split-phase induction motor by using fuzzy-based PID controller," Journal of Electrical Engineering, vol. 70, no. 2, pp. 103–112, Apr. 2019.

[13] S. Bhongade, and V. Parmar, "Automatic Generation Control of Two-Area ST- Thermal Power System using Jaya Algorithm",International Journal of Smart Grid, Vol.2, No.2, 2018.

[14] D. Gueye, A. Ndiaye, M. Tankari, M. Faye, A. Thiam, L. Thiaw, and G. Lefebvre," Design Methodology of Novel PID for Efficient Integration of PV Power to Electrical Distributed Network", International Journal of Smart Grid, Vol.2, No.1,2018.

[15] D. Kumanan and B. Nagaraj, "Tuning of proportional integral derivative controller based on firefly algorithm", Syst. Sci. Control Eng.1, pp. 52-56, Vo. l5, 2013.

[16] A. Hamdy, H. Hasanien and A. Abdelaziz, "Development of Optimal PI Controllers of an Inverter–Based Decentralized Energy Generation System Based on Equilibrium Optimization Algorithm", International Journal of Renewable Energy research', Vol. 11, No. 3, September 2021, pp. 1095-1106.

[17] B. John and K. AlYahya, "Artificial bee colony training of neural networks: comparison with back-propagation, Memetic Comput. Vol. 6, pp. 171–182, 2014.

[18] A. Mishra, A. Khanna, N. Singh, and V.K. Mishra, "Speed control of DC motor using artificial bee colony optimization technique, Univers J. Electr Electr Eng.1, Vol. 3, pp. 68–75, 2013.

[19] M. Gafar, R. A. El-Sehiemy, and H. Hasanien, "A Novel Hybrid Fuzzy-JAYA Optimization Algorithm for Efficient ORPD Solution," IEEE Access, vol. 7, pp. 182078–182088, 2019.

[20] C. Aoughlis, A. Belkaid, I. Colak, O. Guenounou and M. Kacimi, "Automatic and Self Adaptive P&O MPPT Based PID Controller and PSO Algorithm," 2021 10th International Conference on Renewable Energy Research and Application (ICRERA), pp. 385-390, 2021.

[21] E. El Shenawy, M. Kamal and M. Mohamad, "Artificial Intelligent Control of a Solar Tracking System", Journal of Applied Sciences Research, Vol.8, pp. 3971-3984, 2012.

[22] A. Adhim and A. Musyafa, "Optimization of PID Controller Based on PSO for Photovoltaic Dual Axis Solar Tracking in Gresik Location Eastava", International Journal of Engineering & Technology IJET-IJENS, Vol.16, No. 01, pp. 65-71, 2016.

[23] E. Kiyak and G. Gol, "A comparison of fuzzy logic and PID controller for a single-axis solar tracking system", Kiyak and Gol Renewables, Vol.3, 2016.

[24] M. A. Usta, Ö. Akyazi and İ. H. Altaş, "Design and performance of solar tracking system with fuzzy logic controller used different membership functions," *2011 7th International Conference on Electrical and Electronics Engineering (ELECO)*, 2011, pp. II-381-II-385.

[25] S.Iulia, F.Ioana, S.Grigore, A.Nicoleta, and I.S.Sergiu, "Design and implementation of a solar-tracking algorithm", Procedia Eng., Vol. 69, pp. 500–507, 2014.

[26] M. Clifford, and D. Eastwood, "Design of a novel passive solar tracker", Solar Energy, Vol. 77, pp 269-280, 2004.

[27] Z. Xinhong, W. Zongxian, and Y. Zhengda, "Intelligent Solar Tracking Control System Implemented on a FPGA", Institute of Electrical Engineering, Yuan Ze University, 2008.

[28] F.M. Lorilla and R. B. Barroca, "Flexible Dynamic Sun Tracking System (Sts) Employing Machine Vision Control Approach", International Journal of Renewable Energy Research (IJRER), Vol. 12, No. 2, pp. 685-591, 2022.

[29] A. M Yousef, S. A. Mohamed Abdelwahab, Farag K. Abo-Elyousr, and Mohamed Ebeed "Optimization of PID controller for Hybrid Renewable Energy System using Adaptive Sine Cosine Algorithm", International Journal of Renewable Energy Research (IJRER), Vol.10, No.2, pp.669-677, 2020.

[30] A. Heidari, S. Mirjalili, H. Faris, I. Aljarah, M. Mafarja, and H. Chen, "Harris hawks optimization: Algorithm and applications, Future Generation 173 Computer Systems", Future Generation Computer Systems, vol. 97, pp. 849-872, 2019.

[31] R. Devarapalli and B. Bhattacharyya, "Application of Modified Harris Hawks Optimization in Power System Oscillations Damping Controller Design," *2019 8th International Conference on Power Systems (ICPS)*, pp. 1-6, 2019.

[32] J. Yu, C.-H. Kim, and S.-B. Rhee, "The Comparison of Lately Proposed Harris Hawks Optimization and Jaya Optimization in Solving Directional Overcurrent Relays Coordination Problem," Complexity, vol. 2020, pp. 1–22, 2020.

[33] S. Ekinci, D. Izci and B. Hekimoğlu, "PID Speed Control of DC Motor Using Harris Hawks Optimization Algorithm," *2020 International Conference on Electrical, Communication, and Computer Engineering (ICECCE)*, pp. 1-6, 2020.

[34] W. Fu and Q. Lu, "Multi-objective Optimal Control of FOPID Controller for Hydraulic Turbine Governing Systems Based on Reinforced Multiobjective Harris Hawks Optimization Coupling with Hybrid Strategies," Complexity, vol. 2020, pp. 1–17, 2020.

[35] Z. Elkady, N. Abdel-Rahim, A. A. Mansour, and F. M. Bendary, "Enhanced DVR Control System Based on the Harris Hawks Optimization Algorithm," IEEE Access, vol. 8, pp. 177721–177733, 2020.

[36] S S. Ekinci, B. Hekimoğlu and E. Eker, "Optimum Design of PID Controller in AVR System Using Harris Hawks Optimization," *2019 3rd International Symposium on Multidisciplinary Studies and Innovative Technologies (ISMSIT)*, pp. 1-6, 2019.

[37] S. Ekinci, B. Hekimoğlu, A. Demirören and S. Kaya, "Harris Hawks Optimization Approach for Tuning of FOPID Controller in DC-DC Buck Converter," *2019 International Artificial Intelligence and Data Processing Symposium (IDAP)*, pp. 1-9, 2019.

[38] A. Sharma, A. Saxena, S. Shekhawat, R. Kumar, and A. Mathur, "Solar Cell Parameter Extraction by Using Harris Hawks Optimization Algorithm," Studies in Computational Intelligence, pp. 349–379, 2020.

[39] M. A. Mossa, O. M. Kamel, H. M. Sultan, and A. A. Z. Diab, "Parameter estimation of PEMFC model based on Harris Hawks' optimization and atom search optimization algorithms," Neural Computing and Applications,Vol.3, pp. 5555–5570, 2020.

[40] X. Zhang, K. Zhao, and Y. Niu, "Improved Harris Hawks Optimization Based on Adaptive Cooperative Foraging and Dispersed Foraging Strategies", IEEE Access, Vol. 8, pp. 160297 – 160314, 2020.

[41] S. Khalifeh, S. Akbarifard, V. Khalifeh, and E. Zallaghi, "Optimization of water distribution of network systems using the Harris Hawks optimization algorithm (Case study: Homashahr city)", Elsevier, MethodsX, Vol. 7, pp. 1-10, 2020.

[42] Y. M. Alsmadi, A. M. Abdel-hamed, A. Ellissy, A. S. El-Wakeel, A. Y. Abdelaziz, V. Utkin, and A. Uppal, "Optimal Configuration and Energy Management Scheme of an Isolated Microgrid Using Cuckoo Search Optimization Algorithm", the Journal of Franklin Institute, Elsevier, Volume 356, Issue 8, Pages 4191-4214, 2019.

[43] A. M. Abdel-hamed, A. Ellissy, A. S. El-Wakeel, and A. Y. Abdelaziz, "Optimized Control Scheme for Frequency/Power Regulation of Microgrid for Fault Tolerant Operation", Electric Power Components and Systems, Vol. 44, pp.1429–1440, 2016.

[44] D. Gueye, A. Ndiaye, M. Abdou Tankari, M. Faye, A. Thiam, L. Thiaw, and G. Lefebvre,"Design Methodology of Novel PID for Efficient Integration of PV Power to Electrical Distributed Network", International Journal of Smart Grid, Vol. 2, No.1, 2018.